Inclusive electron scattering from ^{2}H, ^{3}He, and ^{4}He

S. A. Dytman
University of Pittsburgh, Pittsburgh, Pennsylvania 15260

A. M. Bernstein, K. I. Blomqvist,* T. J. Pavel, and B. P. Quinn†
Massachusetts Institute of Technology, Cambridge, Massachusetts 02139

R. Altemus, J. S. McCarthy, G. H. Mechtel, T. S. Ueng, and R. R. Whitney‡
University of Virginia, Charlottesville, Virginia 22901

(Received 15 April 1988)

We present new results for inclusive electron scattering in ^{2}H, ^{3}He, and ^{4}He in order to test the reaction mechanism for quasielastic scattering as a function of nuclear density. Radiative corrections are applied to the cross section data and Rosenbluth separations are made for three-momentum transfer (q) between 300 and 600 MeV/c. The A and q dependencies of the data are discussed for the quasielastic peak and the region between the quasielastic peak and the Δ resonance peak (dip region). Comparisons are shown between the data and models based on a quasielastic reaction mechanism. The models give a reasonable representation of the peak at $q \sim 500$ MeV/c, but the longitudinal data for the helium isotopes are significantly suppressed with respect to the quasielastic predictions at $q < 400$ MeV/c. None of the calculations predict the rapid rise with q and A in the transverse strength in the dip region seen in the data. A significant breakdown of the quasielastic picture is seen in the data as A increases from 2 to 4.

I. INTRODUCTION

The lightest nuclei have been important testing grounds for our knowledge of nuclear forces because the small number of interacting particles affords the opportunity to obtain theoretical results with the fewest approximations. Electromagnetic interactions have been especially well suited to provide data that test detailed models because the interaction with nuclei is relatively weak and well known.[1] For example, deuteron threshold electrodisintegration data have been important in showing the existence of meson currents in nuclei.[2] Precise elastic electron-scattering data for the mirror three-body nuclei[3] (^{3}H and ^{3}He) have brought out questions about the relative roles of meson currents and possible signatures of nucleon substructure. Inelastic processes have been studied much less frequently.

Theoretical models have long been applied to calculating the ground-state properties (e.g., binding energies and electromagnetic moments) of ^{2}H, ^{3}H, and ^{3}He. The improved reliability of three-body calculations using Faddeev and variational techniques has recently led to a study of three-body forces[4] in order to explain the binding energies of ^{3}H and ^{3}He. For ^{4}He, there is a more severe problem with underbinding in standard calculations using two-body forces,[5] but the calculations are not as well established as for the three-nucleon system. Techniques for calculating realistic wave functions for four interacting nucleons are being developed by the Urbana-Argonne group.[5]

Inelastic reactions can expand our knowledge because more varied phenomena can be examined.[1,6] For example, it is possible to examine single-particle aspects of the wave function more closely. However, all excited states for these nuclei are unbound, and theoretical calculations in the continuum are more difficult than for elastic reactions. For inelastic reactions in ^{2}H below pion production threshold, reliable calculations can be made because there are only two particles in the final state. However, difficulties with the handling of final state interactions (FSI) away from threshold have prevented the full application of modern three-body techniques to inelastic reactions in ^{3}H and ^{3}He thus far. The problems met in calculations for ^{4}He require further approximations.

In recent years, coincidence cross sections for $(e,e'p)$ with quasielastic kinematics have been published for ^{2}H by Saclay,[7] and for ^{3}He by Saclay[8] and Nationaal Instituut voor Kernfysica en Hoge-Energiefysica (NIKHEF),[9] in order to measure the proton density in momentum space and study the reaction mechanism. Calculations using realistic wave functions that assume a quasielastic reaction mechanism describe that data reasonably well, but only when final-state interactions among the outgoing nucleons are taken into account. The FSI change the results by roughly 20% for ^{2}H at small recoil momentum.[10]

Inclusive cross sections are measured by detecting only the scattered electron in the final state. All kinematically possible nuclear final states are summed over, including one or more nucleon knockout and pion production when the energy is high enough. Thus general properties of the nucleus are sampled in contrast to the specific kinematics sampled by an exclusive measurement such as $(e,e'p)$. There are a number of reasons for studying (e,e') reactions. First, the quasielastic picture should be more accurate since the lowest-order reaction mechanisms will normally contribute most heavily in the (e,e') data. Distortion effects for the electron are calculable and the data

can be corrected for these effects. Secondly, only one particle is detected in the final state, so the measurements take much less beam time. While only carefully selected ranges of kinematics have been studied in $(e,e'p)$ experiments, a single (e,e') experiment can collect data at numerous beam energies and scattering angles. Thus the radiative corrections and separation of cross sections into longitudinal and transverse response functions can be done for (e,e') with minimal model dependence. Finally, since the total inelastic strength is measured, a comparison of results for both (e,e') and $(e,e'p)$ can help disentangle questions about reaction mechanisms.

For electron beams in the energy range of this experiment, the spectrum of inelastically scattered electrons has the features shown in Fig. 1. There, we show the inelastic spectrum (the elastic peak and its radiative tail have been subtracted) for a ^{3}He target taken with a beam energy of 510.2 MeV and the spectrometer set at 60° lab-scattering angle. The prominant peak in the spectrum comes about largely through single-nucleon knockout processes (the peak cross section occurs at energy loss close to that for an electron recoiling from a free nucleon, 109.1 MeV in this case) and is thus called the quasielastic peak. At energy losses higher than those considered in this experiment, a second peak is populated by quasielastic $\Delta(1232)$ production. The region between the peaks is called the dip.

Inclusive electron-scattering data have been published for a variety of nuclei in the range of momentum transfers of 300–600 MeV/c. Rosenbluth separations of longitudinal and transverse contributions were first accomplished in the 1980s for ^{12}C, ^{40}Ca, ^{48}Ca, Fe, and U at Bates[11] and Saclay.[12] Attempts to describe the data with purely quasielastic models met with mixed success. Relativistic Fermi-gas calculations[13] which match cross-section data at kinematics near the quasielastic peak, typically overestimate the longitudinal response function and underestimate the transverse response function. This was surprising since the region near the peak should be predominantly populated by quasielastic processes. A number of explanations have been offered to explain the suppression of the longitudinal strength in nuclei, including final-state interactions,[14] relativistic effects,[15] and nuclear medium modifications of single-nucleon properties.[16] The strength in the dip is largely transverse and much greater than is expected with a purely quasielastic reaction mechanism. This strength has usually been attributed to multinucleon mechanisms. Since much more severe approximations are required to get quantitative solutions using specific models for medium weight and heavy nuclei, a study of very light nuclei is expected to have great value in examining these effects. In particular, the range of densities is quite large in the nuclei studied here; many-body effects can be expected to be much more important in ^{4}He than in ^{2}H.

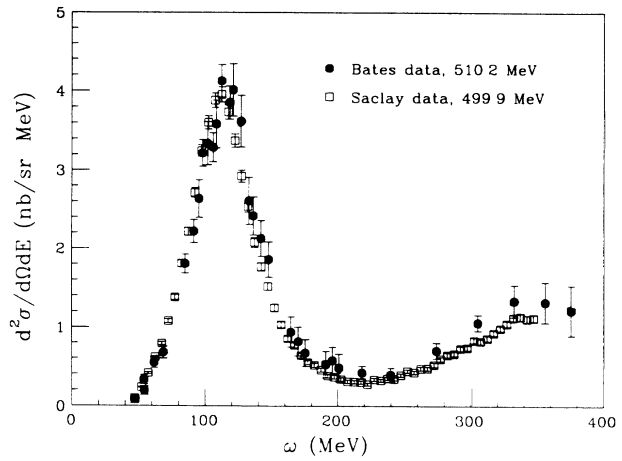

FIG. 1. Fully corrected inelastic cross-section data for a ^{3}He target from this experiment (solid circles) at a beam energy (E_0) of 510.2 MeV and a scattering angle (θ) of 60°. These are compared with data from the Saclay ^{3}He experiment (Ref. 24) (open squares) at $E_0=499.9$ MeV and the same angle. The shift in peak position of about 4 MeV can be accounted for by the difference in beam energy.

The amount of inclusive (e,e') data with radiative corrections published for these light nuclei is nevertheless small. For ^{2}H, unseparated data from Mainz[17] are available for a beam energy of 298.8 MeV at two angles. Purely transverse data at energies of 220, 270, and 320 MeV have been published by the University of Massachusetts.[18] For the kinematic region examined in these experiments, effects involving nucleon degrees of freedom might be expected to dominate and they can be included consistently. For example, nucleon-nucleon FSI effects can be generated with the same potential that is used for the ground-state wave function. Quite detailed theoretical calculations by Laget,[19] and Leidemann and Arenhövel[20] are available. Although the Leidemann and Arenhövel predictions are in excellent agreement with the Mainz cross-section data,[17] the calculations are 5–10% larger than the University of Massachusetts transverse data.[18]

Single inelastic spectra were published for ^{3}He and ^{4}He at 500 MeV incident energy and 60° scattering angle by McCarthy *et al.*[21] in 1976. No calculations have been published for the ^{4}He data, and quasielastic calculations[22,23] with Faddeev wave functions for the ^{3}He data achieve only qualitative agreement. In particular, the strength at the quasielastic peak is overestimated by about 15%.

The data from a recent Saclay experiment published by Marchand *et al.*[24] for ^{3}He agrees well with the McCarthy *et al.* data and greatly extends the range of kinematics studied. The data are presented as longitudinal and transverse response functions at constant four-momentum transfer, $q_\mu^2=-0.1$, -0.15, -0.25, and -0.3 (GeV/c)^2, and have significant overlap with the kinematic region studied in this experiment. Their data are compared with calculations by Laget.[25] These calculations are the first to include all of the known contributing reaction mechanisms for ^{3}He. Nucleon FSI and meson exchange current effects are included in a semiempirical way; pion production is added in a quasielastic formalism. The dip is a complicated combination of all these effects. The calculations are in good agreement with the data only in certain situations. For the data at high

momentum transfer (where higher order effects should be less important), R_L is reproduced well, but the R_T calculation is too large at the quasielastic peak and too small in the threshold region. At lower momentum transfers, the FSI produce a good description of the threshold data, but the height of the quasielastic peak (and the summed strength) is too large in the calculation of both R_L and R_T. In the dip, the data for R_L are quite small in magnitude and the calculations are inside the error bars. On the other hand, the calculations for R_T underestimate the magnitude of the data by roughly 30–40 %. This shortfall in the dip is similar to that obtained for ^{12}C data.[12]

Thus the interpretation of inclusive (e,e') data for very light nuclei at present displays difficulties similar to those seen in the heavier nuclei. At least part of the trouble can be attributed to a lack of comprehensive data for a variety of nuclei. The purpose of this experiment was to provide data for a broad range of kinematics and a number of targets (^{2}H, ^{3}He, and ^{4}He). Here we present and discuss cross section and separated response function data for all targets for momentum transfers in the range of about 270–500 MeV/c. We will emphasize the A dependence data in the quasielastic peak and dip kinematic regions. Although all these nuclei are very light compared to typical nuclei, the number of interacting nucleons and the nucleon density increase rapidly between ^{2}H and ^{4}He. A key issue is whether the data display a corresponding increase in the complexity of the reaction. The ^{2}H data are discussed further in a separate paper[26] because these data can be compared with more detailed calculations.

II. KINEMATICS

The cross section for inclusive electron scattering at beam energy, E_0, scattering angle, θ, and scattered energy, E', is described in terms of the energy loss, $\omega = E_0 - E'$, and the three-momentum transfer (ignoring the mass of the electron)

$$|\mathbf{q}|^2 = E_0^2 + E'^2 - 2E_0E'\cos\theta \ .$$

The mass of the virtual photon (or four-momentum transfer) is

$$q_\mu^2 = -4E_0E'\sin^2(\theta/2) = \omega^2 - |\mathbf{q}|^2 \ .$$

We will also use the symbol q for the three-vector momentum transfer. As with elastic electron scattering, the Born approximation cross section can be written in terms of the Mott cross section, σ_M, and two response functions that depend only on q and ω.

$$\frac{d^2\sigma}{d\Omega\, dE} = \sigma_M(E_0,\theta)\left[\frac{-q_\mu^4}{q^4}R_L(q,\omega) + \left[\frac{-q_\mu^2}{2q^2} + \tan^2\theta/2\right]R_T(q,\omega)\right] ,$$

where

$$\sigma_M = \frac{\alpha^2}{4E_0^2}\frac{\cos^2\theta/2}{\sin^4\theta/2} \ .$$

$R_L(q,\omega)$ results from the absorption of longitudinally polarized virtual photons and $R_T(q,\omega)$ from transverse polarized virtual photons. A Rosenbluth separation into R_L and R_T can be made by taking data at the same q and ω, but different E_0 and θ. In inclusive scattering measurements, all possible final states are summed; thus, the only kinematic restrictions are that $\omega^2 < q^2$ in (e,e') and that target recoil determines the minimum ω for a given E_0, θ, and target. The data sample a triangular region in the ω vs q plane as shown in Fig. 2. To obtain separated response functions across the quasielastic peak ($\omega \sim |q_\mu|^2/2M_N$; M_N = nucleon mass) for 300 MeV/c $< q <$ 500 MeV/c, data were taken at 60° for five beam energies from 292.8 to 596.8 MeV, and at 134.5° for six beam energies from 174.3 to 444.2 MeV. As a check, data were also taken at 90° scattering angle for 223.8 and 287.8 MeV beams.

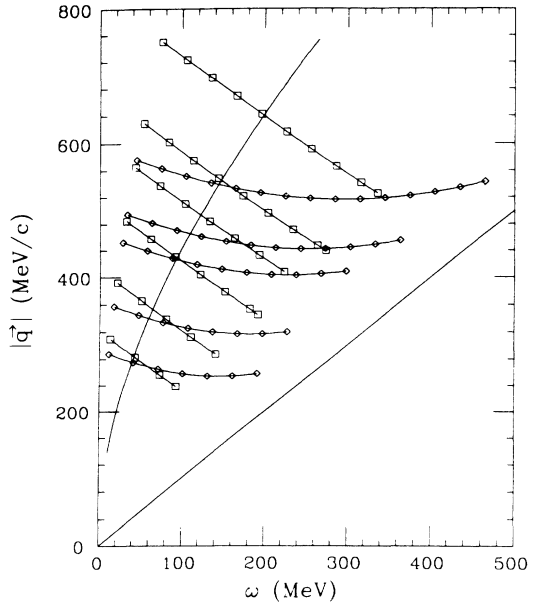

FIG. 2. Kinematics for this experiment. The locus of points covered at the various beam energies and scattering angles is shown in terms of the energy loss (ω) and momentum transfer (q). Forward-angle kinematics (60°) are shown as diamonds and back-angle kinematics (134.5°) are shown as boxes joined by solid lines. The solid line cutting across these lines shows the kinematics for elastic electron-nucleon scattering. The diagonal line shows the real photon limit, $q = \omega$.

III. EXPERIMENT

A brief description of our experimental methods will be given here. The reader is directed to Refs. 26 and 27 for a more complete discussion.

The experiment was done at the Bates Linear Accelera-

tor Center using the ELSSY spectrometer to detect the scattered electrons. Separate cylindrical gas target cells were filled with ^{1}H, ^{2}H, ^{3}He, and ^{4}He to a pressure of about 100 atm at room temperature, and sealed. Along with an evacuated cell, all target cells were placed on a target ladder and cooled to liquid-nitrogen temperatures. Thus the target geometry and radiator configurations were the same for all data presented here. Target windows were 0.51 mm thick #304 stainless steel, except for the endcaps which were 0.25 mm. Small areas ($\sim$6.4 mm diameter) of the endcaps where the main beam passes through, were electropolated with 0.05 mm copper to improve the thermal conductivity of the material the beam heats directly. The remainder of the endcaps were coated with 0.25 mm copper. Two sets of horizontal slits ensure that none of the electrons scattered in the gas hit the spectrometer pole faces, and that none of the electrons scattered in the end caps have a direct path into the spectrometer.

The beam was tuned to a circular spot with a diameter of about 2.4 mm. Data were taken at thirteen different energies (174–597 MeV) divided among three spectrometer angels (60°, 90°, and 134.5°). At each energy-angle combination, the inelastic spectrum was scanned by the spectrometer (6% momentum bites) down to about 80 MeV scattered electron energy. Depending on the beam energy, from ten to fifteen spectrometer settings were required. At each setting, data was taken with each of the four gas targets and with the empty target cell.

There are numerous potential sources of background in inclusive experiments. In general, the problems are easy to overcome near the quasielastic peak where the energy loss is relatively small and the true cross sections are large. However, in the "dip" region, more energy is available for background processes and the true cross sections are smaller. Pions and muons passing through the spectrometer were vetoed by requiring a signal in an aerogel Cerenkov detector ($n=1.05$). Most electrons from double scattering processes (e.g., hard bremsstrahlung in the window followed by scattering in the side of the target) were measured in the data taken with the empty target and then subtracted from the raw data. In the direction along the beam line, it was possible to accurately determine the source of each event. This proved to be a very effective means of detecting and subtracting any remaining backgrounds.

IV. DATA ANALYSIS

The thirteen separate spectra for each target gas were handled in the same way. The energy spectrum at each spectrometer setting was divided into three double-differential cross-section bins except in cases where statistics were low and only one bin was used. The blank target data were scaled and subtracted, channel by channel. The radiation tail from elastic scattering was calculated and subtracted from each spectrum.[27] At a number of beam energies, spectra were also measured with the spectrometer set for positive particles. Since the aerogel Cerenkov detector vetoed all particles heavier than electrons, these spectra contain only pair-produced positrons and nontarget-related background. In previous experiments,[11,12] these events have been subtracted from the electron spectra, assuming an equal number of pair-produced electrons. Pair-production cross sections[29] are proportional to Z^2+Z and are thus a much smaller contribution in these experiments on light nuclei than has been the case in most inclusive data. Our calculations using the formulas in Ref. 29 predict a negligible number of true pair-production events in our spectra, and so no subtraction was made. Unfortunately, these calculations could not be verified with the positive data. Using ray-tracing methods, it was established that few of the accepted events had the characteristics of valid events and cross sections could not be reliably extracted.

The correction methods for bremsstrahlung processes followed the work of Mo and Tsai.[28] A full account is given in Refs. 26 and 27. To subtract radiative tails from an inelastic spectrum, cross sections must be known for all lower beam energies that can contribute at each value of ω. For these data, cross sections were interpolated to other beam energies by y-scaling (with phenomenological modification of y) at the quasielastic peak and by constant recoil mass above the pion production threshold. All the data for each target, except ^{1}H, were corrected iteratively at each angle until a stable approximation to the true cross sections was obtained. Typical corrections for data at the quasielastic peak were about 30%. An important check on the calculation of radiative corrections was available in comparisons with the ^{1}H inelastic spectra. For ω less than the minimum energy required for pion production, the contribution from bremsstrahlung processes in the elastic channel can be both measured (a range of $\sim$150 MeV) and independently calculated[28] because elastic scattering is the only open channel. These parameter-free calculations achieved good agreement with all the hydrogen data (see Refs. 26 and 27 for examples). (This is also a good verification of proper background subtraction, because it is highly unlikely that undetected background could make up for any deficiencies in the radiation tail calculations in all thirteen hydrogen spectra measured.)

The absolute normalization of these data is well established. Elastic data for all targets were taken at most beam energies and are consistently about 6% less than smooth fits to existing elastic data.[26] All cross sections were multiplied by 1.06 and a 3% systematic error was folded into each estimated error to account for possible errors in absolute normalization.[27]

With the resulting double-differential cross sections, a comparison can be made between this experiment and the Saclay ^{3}He experiment.[24] In Fig. 1, we show fully corrected inelastic energy spectra at 60° from Saclay at 499.9 MeV beam energy and from this experiment at 510.2 MeV. There is a systematic shift in the position of the quasielastic peak of about 4 MeV, consistent with the difference in energy loss for elastic electron-nucleon scattering between the two beam energies. Outside of this known effect, the agreement of the two sets is very good.

Figures 3–5 show the cross sections for all targets at three beam energies (596.8, 465.3, and 292.8 MeV) for the

forward angle (60°). The data points include both random and systematic errors. All spectra are dominated by the quasielastic peak. The peak of the cross section is symmetric and is centered at values of ω close to where the hydrogen elastic-scattering peak would occur except for ^{4}He at low q; the width of the peak grows with A, reflecting the increase in average nucleon momentum in the nuclear ground state. For ^{4}He at low q (e.g., Fig. 5), the peak is shifted to lower energy loss and is quite asymmetric. These effects could be due to an enhancement in these spectra from FSI or excitation of the broad inelastic states in ^{4}He between 20 and 30 MeV excitation energy. The summed inelastic cross section in the peak at each energy grows roughly linearly with A at the back angle, reflecting dominance of the transverse channel and the incoherent nature of the basic reaction. Although the beginning of the Δ quasielastic peak can be seen in some of the spectra, none of the spectra obtained in this experiment show the full Δ peak. In the dip, the data are largely transverse and grow rapidly with both A and q. The dependence of R_T in the dip on q and A for all three targets is roughly given by a power law, $R_T \sim q^{1.4} A^{1.7}$. For both the q and A dependence, the data for heavier nuclei[12] increase much less rapidly (roughly linearly) than is seen for these light nuclei. At 444.2 MeV and 134.5°, the dip cross section is almost as large as at the quasielastic peak for ^{4}He.

The Rosenbluth separations were performed along the q-ω curves corresponding to constant incident energy for a scattering angle of 134.5° (see Fig. 2). By choosing incident energies where the back-angle data of this experiment were taken, no interpolation of that data was required. The forward-angle data had to be interpolated to the values of q and ω corresponding to the back-angle data. This was done in the same way as for the radiative corrections. Errors were propagated into the final results according to Gaussian statistics. Separated response functions at the kinematics of the back-angle points are shown in Figs. 6–8 for beam energies of 233.1, 327.7, and 444.2 MeV, respectively. Because of propagation of errors in the interpolations required, the response function data have somewhat larger error bars than the cross-section data. At the highest energy where separations are shown (444.2 MeV), we were unable to take the forward-angle data required to get both R_L and R_T because the necessary beam energy of 800 MeV was unavailable. However, the 444.2 MeV back-angle data is almost entirely transverse, so R_T can be obtained by using a good estimate of R_L to make the required $\sim$4% correction. In this case, we used the calculation of the Rome group.[30] Where more than one calculation was available, we verified that the extracted R_T values were independent of the calculation chosen. In all figures, we show the q variable along the top axis of each figure. Tables of all data points can be obtained from the authors.

V. COMPARISON WITH A SIMPLE QUASIELASTIC MODEL

The dominance of the spectra by the quasielastic peak suggests that it would be instructive to compare the data

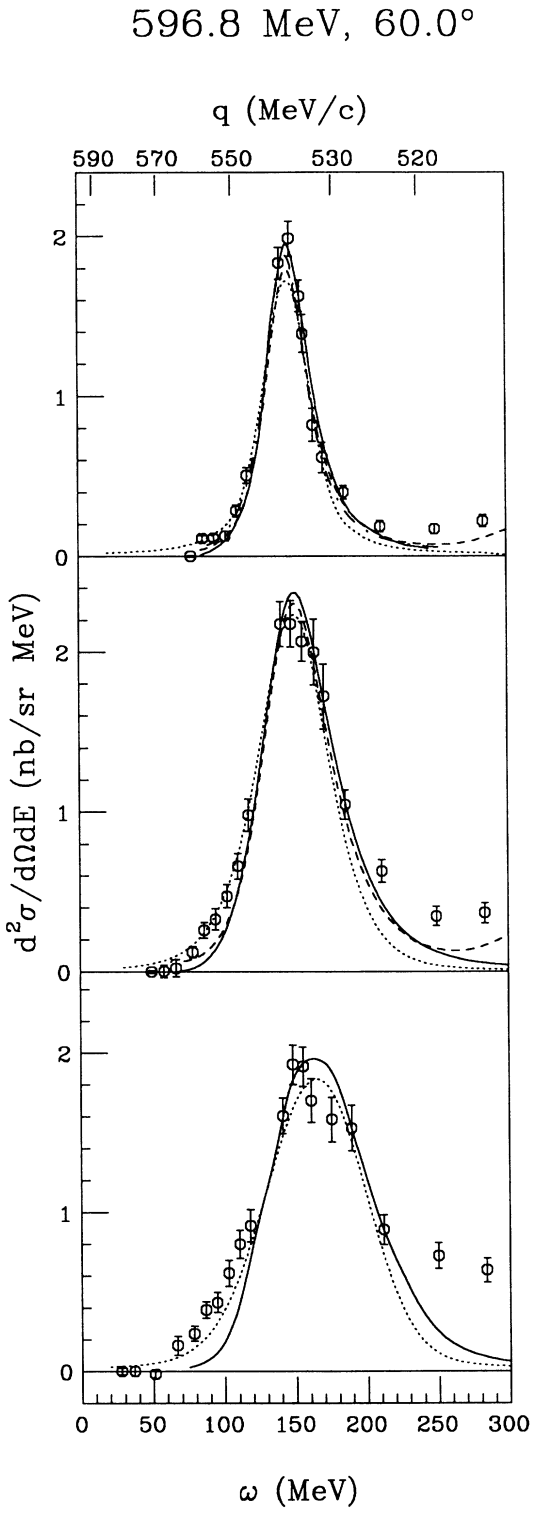

FIG. 3. Cross-section data for all three targets are shown for $E_0 = 596.8$ MeV and $\theta = 60°$. The data are shown in the order of ^{2}H, ^{3}He, and ^{4}He from top to bottom. Error bars that include all random and systematic sources are displayed. Calculations are shown for ^{2}H by Arenhövel (solid), Laget (dashed), and Ciofi degli Atti *et al.* (dot-dash). For ^{3}He and ^{4}He, the solid line represents the calculation of Ciofi degli Atti *et al.* Laget's prediction (^{3}He only) is shown as a dashed line; the simple quasielastic prediction is shown for all three targets as a dotted line.

with a simple quasielastic model.[31] An analysis of this type tests the importance of a single reaction mechanism (quasielastic nucleon knockout) and gives a common ground for discussing the large amount of data reported here. The most quantitative statements will, of course, be made with regard to more exact models such as those discussed in the Introduction, but only models with strong quasielastic assumptions can presently make predictions for all few-body targets at the same level of approximation. To carry out inelastic calculations, technical difficulties in describing the final state require the use of a simpler reaction model than is the norm in elastic-

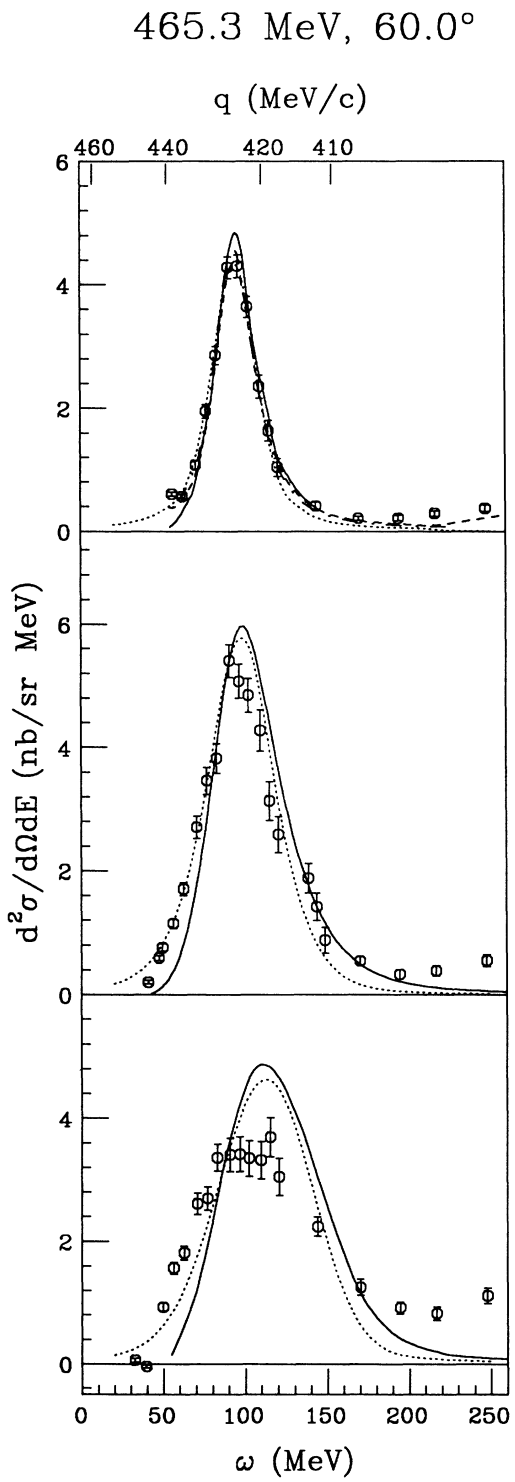

FIG. 4. Cross-section data for all three targets are shown for $E_0=465.3$ MeV and $\theta=60°$. Calculations are represented in the same way as Fig. 3.

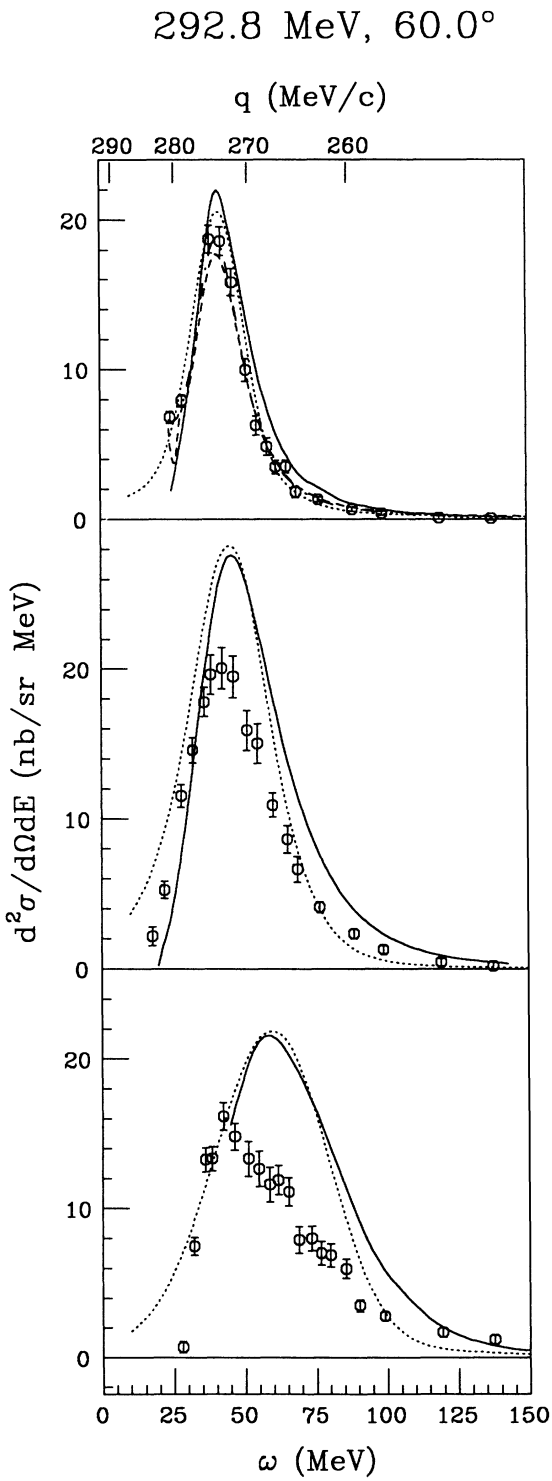

FIG. 5. Cross-section data for all three targets are shown for $E_0=292.8$ MeV and $\theta=60°$. Calculations are represented in the same way as Fig. 3.

scattering models. The assumptions necessary for a ^{2}H calculation are much better understood than those required for ^{4}He due to the rapid growth in complexity of the final state with A.

We will present results obtained from a model based on the work of Moniz.[31] In that paper, expressions are given for the cross section and the response functions in terms of integrals over the nucleon momentum distribution. The electron-nucleus interaction is taken to be an incoherent sum of the cross sections for scattering from each of the bound nucleons. The eN form factors are taken to be the same for bound as for free nucleon (fit 8.2 of Höhler *et al.*[32] is used in the calculations shown here) but the kinematics take into account the Fermi momentum of the struck nucleon. Pauli blocking for the outgoing nucleon is included. The knowledge of q and ω, the virtual photon momentum and energy, and the requirement of a single ejected nucleon fixes the initial component of the struck nucleon momentum parallel to q. This is a lower bound on the magnitude of the initial nucleon momentum on which the virtual photon can be absorbed,

$$k_{\min}=\left|\frac{2\omega M-q^2}{2q}\right| .$$

In this model, the peak inelastic cross section occurs at values of q and ω for which a nucleon initially at rest in the nucleus can be ejected. The width of the quasielastic peak is determined by the nucleon momentum distribution in the initial nucleus. For events on the low (high) ω side of the peak, the struck nucleon was moving toward (away from) the virtual photon.

These models were originally applied to heavier nuclei with a Fermi gas model for the nucleon momentum distribution, but that would be grossly inadequate for such light nuclei. We have, therefore, used realistic momentum densities calculated by Ciofi degli Atti, Pace, and Salme,[33] and by the Urbana-Argonne group.[5] The calculations are done at an effective energy loss which is smaller than the actual value by a fixed energy that can be thought of as accounting for the average binding energy of the ejected nucleon. Values for this energy shift parameter were set at the separation energies 2, 5.5, and 19.8 MeV for ^{2}H, ^{3}He, and ^{4}He, respectively.

In Fig. 9 we show the predictions for ^{4}He at 510 MeV beam energy and 60° scattering angle compared with $k_{\min}$, the minimum nucleon momentum that can contribute to the cross section in this model. In the tails, only very high momentum nucleons can participate in the reaction, and the single-nucleon contribution to the cross section is then quite small. More complicated reaction mechanisms should be found to be important here.

Calculations from this simple quasielastic model, using the Rome momentum densities, are compared with the data of this experiment in Figs. 3–5. In Fig. 3, data are shown for the three targets at 597 MeV beam energy, and 60° scattering angle. At this beam energy and scattering angle, the cross sections due to the longitudinal and transverse response functions are about equal. The momentum transfer is about 540 MeV/c at the quasielastic peak. The peak is seen to shift to higher ω and be-

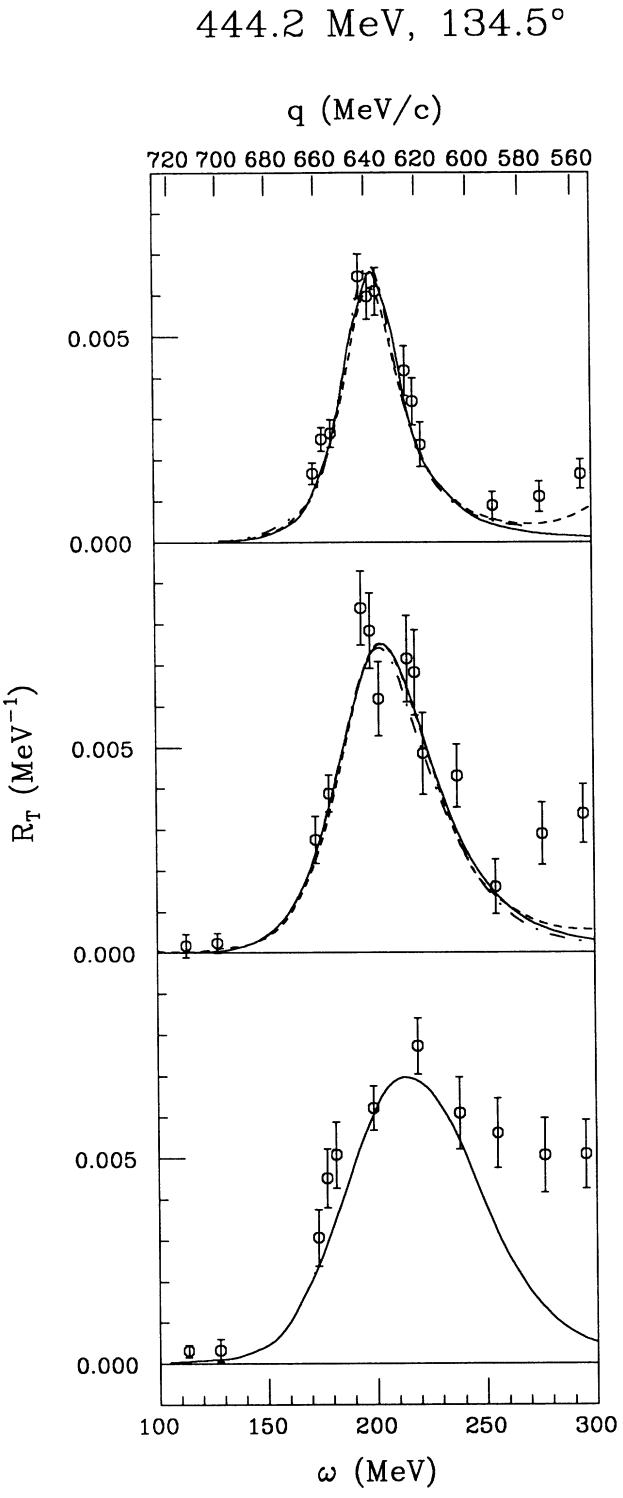

FIG. 6. Transverse response function data (R_T) for this experiment at the kinematics corresponding to the back angle (134.5°) at $E_0=444.2$ MeV. The data are arranged in the order ^{2}H, ^{3}He, and ^{4}He from top to bottom. Calculations are shown for ^{2}H by Arenhövel (solid), Laget (dashed), and Ciofi degli Atti *et al.* (dot-dash). For ^{3}He and ^{4}He, the solid line represents the calculation of Ciofi degli Atti *et al.* Laget's prediction (^{3}He only) is shown as a dashed line and Hajduk (^{3}He only) is shown as a dot-dash line.

come wider as the target atomic weight increases, as predicted by the model based on our knowledge of nucleon binding energies and momentum distributions. However, the calculated width of the peak for ^{4}He is too small and the strength in the dip region for all nuclei in this experiment is underestimated by an amount that grows with A. For ^{4}He, the discrepancy in the dip is similar to what is seen for heavier targets.[13]

At the energy loss where the cross section peaks, the sensitivity to different momentum distributions is of interest. The differences are the most significant for ^{4}He. In Fig. 9 we show the simple quasielastic calculation for

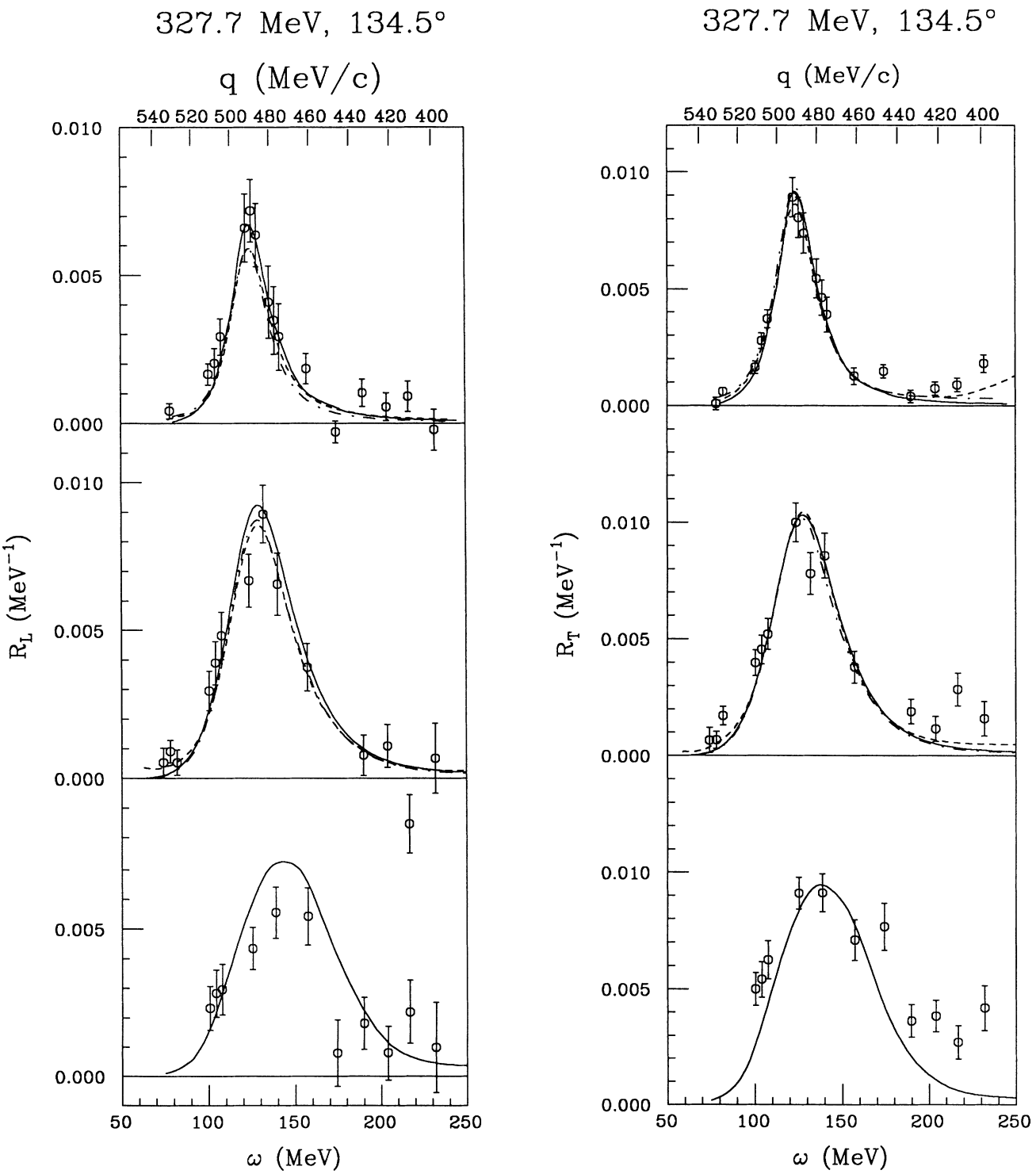

FIG. 7. Longitudinal (R_L) and transverse (R_T) response function data for this experiment are shown in (a) and (b), respectively, at the kinematics corresponding to the backangle (134.5°) at $E_0 = 327.7$ MeV. Calculations are represented by the same symbols as in Fig. 6.

the inelastic cross section at 510.2 MeV beam energy and 60° scattering angle using predictions for the momentum density by the Urbana-Argonne[5] and Rome[33] groups. The Urbana-Argonne group gives densities calculated with two prescriptions for the three-body force that give noticeably different predictions. There is a difference of about 10% due to momentum density sensitivity.

The simple quasielastic model (and the more quantitative models, also) is much less successful in reproducing the data at lower momentum transfers. The data for 292.8 MeV beam energy and 60° have $q = 280$ MeV/c at the quasielastic peak, which is still somewhat larger than

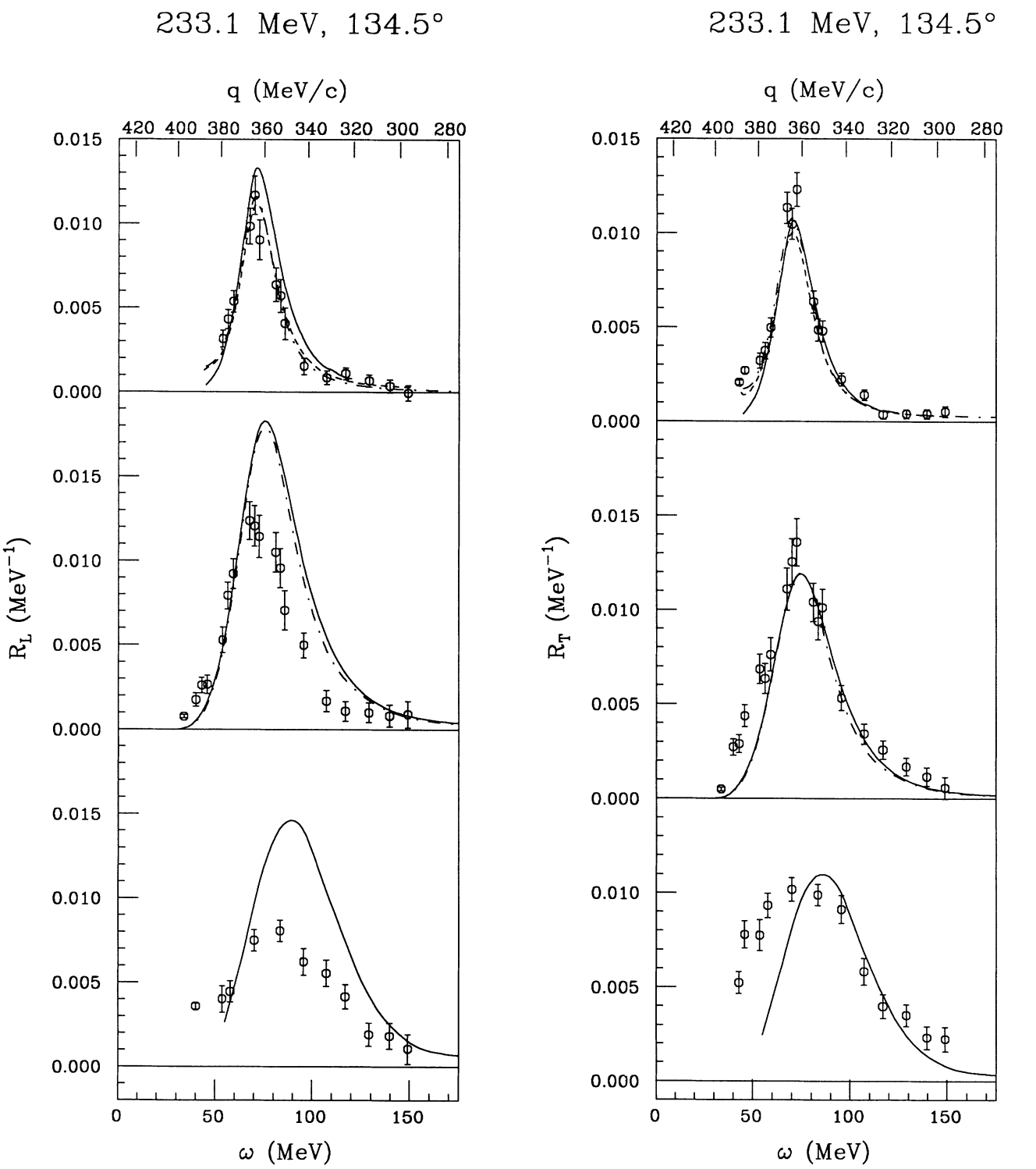

FIG. 8. Longitudinal (R_L) and transverse (R_T) response function data for this experiment are shown in (a) and (b), respectively, at the kinematics corresponding to the backangle (134.5°) at $E_0 = 233.1$ MeV. Calculations are represented by the same symbols as in Fig. 6.

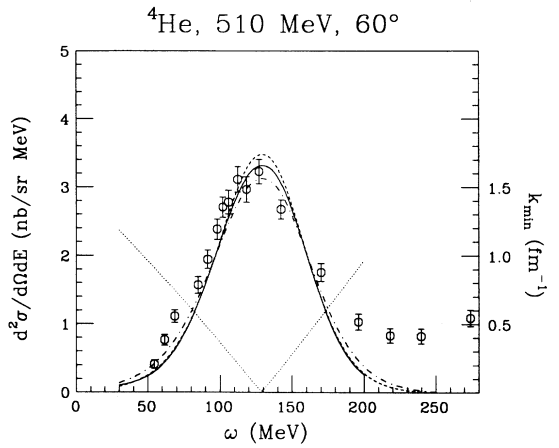

FIG. 9. The cross-section data of this experiment at $E_0 = 510.2$ MeV and $\theta = 60°$ is compared with the results of the simple quasielastic calculation using the momentum distributions of the Rome group (solid) and the Urbana-Argonne group (dashed and dot-dashed) corresponding to the momentum distributions shown. We also show the minimum nucleon momentum (dotted line) that is kinematically allowed to contribute to the cross section in the simple quasielastic model. The scale for this curve is at the right side.

the average nucleon momentum for these light nuclei. Although Pauli blocking effects are not expected to be important, the outgoing nucleon momentum is low enough that FSI can be influential. A quasielastic peak is seen for all three nuclei, but the peak has a significant asymmetry for ^{4}He and the calculations predict a magnitude that is too large. In Fig. 5 we compare these data with the simple quasielastic model predictions and the disagreement is quite significant. A quantitative description of these data will require a significant alteration of the single nucleon knockout picture.

VI. COMPARISON WITH REALISTIC MODELS

A number of quantitative calculations are shown in Figs. 3–8. As discussed in previous sections, the difficulty in performing an accurate and consistent calculation increases greatly from ^{2}H to ^{3}He to ^{4}He. Thus the ^{2}H calculations include the most complicated reaction mechanisms in the most consistent manner. Both Laget and Arenhövel include FSI and meson exchange current (MEC) effects, and Laget also includes incoherent real pion production. For ^{3}He, Laget handles the same effects as in his ^{2}H calculations, but more approximations are required. Only the Rome group has provided results for all three nuclei, but they consider only the quasielastic reaction mechanism. Sauer and collaborators have results for ^{3}He only, again with only the quasielastic reaction mechanism. The ^{2}H calculations are included in the figures for completeness, but are only discussed briefly. A more complete discussion can be found in Ref. 26.

A. Models for ^{3}He and ^{4}He

The calculations of Ciofi degli Atti, Pace, and Salme[30] (see Figs. 3–8), and Hajduk and Sauer[23] (Figs. 6–8), make a direct connection with the single-nucleon spectral function $P(k,E)$ where k and E are the missing momentum and energy for the $A(e,e'N)B$ reaction. In the plane-wave impulse approximation (PWIA) picture, these quantities are the momentum and energy of the struck nucleon in the original nucleus. The spectral function must be calculated separately for each possible final state. For ^{2}H, there is only one possibility (pn), while for the ^{3}He, there are two (ppn and pd) and for ^{4}He, there are five final states ($ppnn$, p^3H, n^3He, pnd and dd) that should be considered. The inclusive (e,e') cross section is obtained by integrating over both nucleon momentum and removal energy

$$\frac{d^2\sigma}{d\Omega_2 dE_2} = 2\pi \sum_{N=1}^{A} \int dE \int k\, dk \left| \frac{\partial \omega}{\partial k} \right|^{-1} \sigma_{eN} P_N(k,E) ,$$

where the ranges of E and k are determined from q and ω and the allowed nuclear states.[30] The two possible final states for $A = 3$ nuclei are treated separately.

The calculations by Laget[25] explore the role of higher-order processes for the ^{3}He target in a diagrammatic approach. Faddeev wave functions[34] are used for the ground-state wave function and the two possible final states are treated separately. Interactions between nucleons in the final state are included in terms of the phase shifts of the lowest partial waves[25] and a quasideuteron model is used for the meson exchange current contributions. In Ref. 25, Laget compares his purely quasielastic prediction with the prediction including FSI and MEC at $q_\mu^2 = -0.2$ (GeV/c)^2, (corresponding to $|q| \sim 460$ MeV/c at the quasielastic peak). There, the additional effects are seen mostly in the tails of the quasielastic peak. For both R_L and R_T, the response is increased near threshold, as is expected since the outgoing nucleons are at low relative momentum where they have strong attraction. The high ω side of the quasielastic peak is enhanced for R_T (presumably, the effect of pion MEC). However, the effects are quite small at the quasielastic peak, resulting in a small enhancement for R_T and almost no effect for R_L. Thus the combined effect of FSI and MEC is generally an enhancement. This produces somewhat better agreement in the tails, but poorer agreement at the quasielastic peak. Because of poor agreement with the Saclay ^{3}He data[24] at the quasielastic peak, a $1/M^3$ relativistic correction to the transverse current is added in Laget's calculations (a 5–15% effect in R_T) shown here.[35] Although all the calculations are in close agreement at the quasielastic peak, the reasons appear to be partly due to a cancellation in Laget's higher-order effects.

B. ^{2}H

The influence of higher-order effects should rise with increasing nuclear density and increasing atomic weight. From both these criteria, ^{2}H data should be easiest to calculate satisfactorily. Calculations with and without FSI or MEC differ by ~5% in either Laget's or Arenhövel's results, an amount comparable to or smaller than the error bars of these data. The calculated values are small in the dip, at most ~15% of the quasielastic peak height,

typically much smaller. The agreement of the calculations with data is quite good, except at the lowest momentum transfers where the height of the quasielastic peak for R_T is underestimated by about two standard deviations. At the 5–10 % level, these calculations very accurately represent these ^{2}H data. The University of Massachusetts R_T data[18] are systematically higher than both these calculations and the data presented here.

C. ^{3}He

For the case of ^{3}He, Figs. 3–5 show that the Rome calculations[30] are much closer to the data at the higher energies. For 596.8 MeV, 60° ($q \sim 540$ MeV/c at the peak), the calculations are a little low at threshold and about 30% low in the dip, but the region near the peak is accurately described. At a beam energy of 292.8 MeV and 60° ($q \sim 275$ MeV/c at the peak), the quasielastic peak in the calculation has approximately the same shape as the data, but it is shifted by about 10 MeV and about 30% larger in magnitude. Separations at comparable momenta are shown in Figs. 6–8 together with both Rome and Hannover calculations. At $E_0 = 327.7$ MeV and a scattering angle of 134.5° ($q \sim 500$ MeV/c at the peak), both R_L and R_T are reasonably well described except in the dip. However, at the lowest q ($E_0 = 233.1$ MeV, $\theta = 134.5°$, Fig. 8) we see that the problems for ^{3}He in the 292.8 MeV cross section are largely in R_L. Both calculations are significantly larger than the data in magnitude for R_L and perhaps slightly smaller for R_T. Good agreement in both R_L and R_T at $q \sim 500$ MeV/c presumably means the single-nucleon effects are being treated accurately in these calculations. No change in the momentum distributions could decrease the low q data without destroying the agreement at high q.

Laget's results for ^{3}He are shown in Figs. 3, 6, and 7. These figures contain the highest q data, and the good agreement among the calculations indicates a minor role for Laget's many-body effects at these kinematics. It would be very interesting to see the role of FSI at the lower momentum transfers. The experimental transverse response function rises rapidly with q in the dip. Although Laget's predictions in the dip are larger than those in either Rome or Hannover, they do not increase with q as rapidly as the data.

D. ^{4}He

Progress in the three-body problem has been spurred by the Faddeev equations, which offer the possibility of a fairly exact wave function. There has been substantial progress in determining the ^{4}He wave function with variational Monte Carlo methods,[5] but these methods have not been applied directly to inelastic processes as yet. Consequently, only the Rome[30] and simple quasielastic calculations are available for the ^{4}He data at this time.

Our data for ^{4}He have poorer statistics than for ^{2}H and ^{3}He, but the disagreements between calculations and data are more pronounced. For the quasielastic peak, the calculations are closest to the data at high q. At low q, both the shape and magnitude of the calculations are wrong. Because of the strong quasielastic assumptions of the Rome model, the predicted shape of the peak changes slowly with q, but the data have quite different shape in the 233.1 MeV separations than at the higher energies. The peak in the data for both R_L and R_T is significantly wider and there is more strength at low ω than what is predicted.

VII. DISCUSSION AND CONCLUSIONS

We have presented data for the quasielastic peak and dip region for momentum transfers from about 300 MeV/c to 600 MeV/c for ^{2}H, ^{3}He, and ^{4}He. The total inelastic cross section for each nucleus roughly follows the average elastic electron-nucleon cross section as a function of beam energy and scattering angle. The peak cross section in each spectrum comes at a value of energy loss close to the value corresponding to elastic scattering from a free nucleon. The peaks widen and shift to higher energy loss as A and q increase. Much of the A dependence of the shift and width reflects the average nucleon separation energy and average nucleon momentum of the target nuclei, respectively, but higher-order reaction mechanisms also populate the tails and affect these quantities. For quasielastic nucleon knockout and increasing q, the virtual photon is less likely to be absorbed on a nucleon with a very small component of momentum along the direction of q and more likely to be absorbed on a moving nucleon. A simple quasielastic[31] model reproduces these qualitative features of the data as do the more realistic quantitative models.

In the dip, the data is primarily transverse and rises quite rapidly with both A and q, roughly by $q^{1.4}A^{1.7}$. The initial nucleon momentum required for the quasielastic reaction mechanism to contribute in the dip is quite large, and all the quasielastic models significantly underestimate the strength. Thus the data suggest that the contribution to the cross section due to multinucleon processes increases rapidly as the number of target nucleons increases from two to four. This is in contrast to the situation for nuclei with $A \geq 12$, where the A dependence is close to linear. Although the most detailed models for both ^{2}H (Arenhövel[20] and Laget[19]) and ^{3}He (Laget[25]) are all too small in the dip region, the discrepancies are larger for ^{3}He.

In the range of momentum transfer of this experiment, the cross sections at threshold are generally larger than the predictions of the quasielastic models. For ^{2}H, a shoulder is seen in some of the spectra and is generally predicted by the models that include nucleon-nucleon FSI. For ^{3}He, only Laget's calculations include FSI. The pure quasielastic calculations are often lower than the data near the inelastic threshold; for the cases where Laget's calculations are available, most of the required strength has been generated.

The accuracy of the calculations at the quasielastic peak varies greatly with A and q. For each nucleus, all models reproduce the qualitative features of the data at high q. However, the gap between the calculations and the data worsens as the momentum transfer decreases; the worsening is much more noticeable in R_L vs R_T and

for ^{3}He and ^{4}He vs ^{2}H. In general, the calculations match the ^{2}H data quite well, while the overall strength for the helium isotopes is significantly overestimated in the longitudinal response function (R_L) at our lowest momentum transfers ($q \sim 350$ MeV/c). The transverse strength of the calculations is in good agreement with the data for ^{3}He and too small for ^{4}He. It is clear that significant modifications to the quasielastic picture of the models presented here will be required at the low momentum transfers for the helium isotopes, even where the cross section is at its maximum in each inelastic spectrum. The discrepancies in heavier mass nuclei are similar, giving evidence that the breakdown of the quasielastic model occurs between $A=2$ and $A=4$. Although estimates of higher order effects for ^{3}He and ^{4}He at lower momentum transfers will ultimately be more reliable than for heavier nuclei, none are available at this time.

Important pieces of physics are not included properly in the quasielastic calculations for the helium isotopes. First, all of the calculations assume a final state composed of only plane-wave knockout states. Thus elastic scattering is not accounted for and the calculated inelastic Coulomb sum rule[36] (the integrated longitudinal inelastic strength) is too large at low momentum transfers. Secondly, multinucleon effects are not handled consistently. The Arenhövel and Laget calculations for the ^{2}H data show that these effects are small and accurately treated for that nucleus, as might be expected for such a diffuse system. With the small increase in A to the helium isotopes (but large increase in average density), these effects should become more important.

Progress is being made in theoretical calculations. Schiavilla *et al.*[37] have recently studied inelastic reactions in ^{3}He, ^{3}H, and ^{4}He with a variational Monte Carlo model. They achieve good agreement for the inelastic Coulomb sum of ^{3}He obtained from the Saclay data[24] down to about 210 MeV/c, implying that the initial state effects are being handled correctly. Work is in progress by the same group[37] on calculations for the response function, examining the role of correlations in the final state. On the experimental side, we have recently taken new data[38] for ^{2}H, ^{3}H, ^{3}He, and ^{4}He for a broader range of momentum transfer. With the new data, we will be able to examine the issues raised in this paper in greater detail.

ACKNOWLEDGMENTS

We wish to thank Dr. J. Flanz and Dr. P. Sargent of MIT-Bates for providing the high-energy beams necessary for accumulating these data. Thanks are also due to Dr. H. Arenhövel, Dr. J. M. Laget, Dr. C. Ciofi degli Atti, Dr. H. Hajduk, and Dr. P. Sauer for providing calculations for our kinematic conditions. Partial support was provided by the National Science Foundation under Contract PHY8518521 and the U.S. Department of Energy under Contract No. DE-AC02-76ER03069.

---

*Present address: Physics Department, Lund Institute of Technology, Lund, Sweden.

†Present address: Physics Department, Carnegie-Mellon University, Pittsburgh, PA 15213.

‡Present address: CEBAF, Newport News, VA 23606.

[1] B. Frois and C. Papanicolos, Ann. Rev. Nucl. Part. Sci. **37**, 133 (1987).

[2] S. Auffret *et al.*, Phys. Rev. Lett. **55**, 1362 (1985).

[3] F. P. Juster *et al.*, Phys. Rev. Lett. **55**, 2261 (1985); D. H. Beck, *ibid.* **59**, 1537 (1987); **59**, 2388(E) (1987).

[4] C. R. Chen, G. L. Payne, J. L. Friar, and B. F. Gibson, Phys. Rev. C **33**, 1740 (1986); J. L. Friar, B. F. Gibson, and G. L. Payne, Ann. Rev. Nucl. Sci. **34**, 403 (1984).

[5] R. Schiavilla, V. R. Pandharipande, and R. B. Wiringa, Nucl. Phys. **A449**, 219 (1986).

[6] Z. Meziani, Nucl. Phys. **A446**, 113c (1985).

[7] M. Bernheim *et al.*, Nucl. Phys. **A365**, 349 (1981); S. Turk-Chieze *et al.*, Phys. Lett. **142B**, 145 (1984).

[8] E. Jans *et al.*, Phys. Rev. Lett. **49**, 974 (1982); Nucl. Phys. **A475**, 687 (1987).

[9] P. H. M. Keizer *et al.*, Phys. Lett. **157B**, 255 (1985).

[10] W. Fabian and H. Arenhövel, Nucl. Phys. **A314**, 253 (1979); H. Arenhövel, *ibid.* **A384**, 287 (1982).

[11] M. Deady *et al.*, Phys. Rev. C **28**, 631 (1983); C. C. Blatchley *et al.*, *ibid.* **34**, 1243 (1986).

[12] P. Barreau *et al.*, Nucl. Phys. A **402**, 515 (1983); Z. E. Meziani *et al.*, Phys. Rev. Lett. **54**, 1233 (1985).

[13] J. W. Van Orden and T. W. Donnelly, Ann. Phys. (N.Y.) **131**, 451 (1981).

[14] A. Dellafiore, F. Lenz, and F. A. Brieva, Phys. Rev. C **31**, 1088 (1985); R. Rosenfelder, Nucl. Phys. **A459**, 452 (1986).

[15] G. Do Dang and Pham Van Thieu, Phys. Rev. C **28**, 1845 (1983).

[16] J. V. Noble, Phys. Rev. Lett. **46**, 412 (1981); L. S. Celenza, A. Rosenthal, and C. M. Shakin, Phys. Rev. C **32**, 248 (1985); P. J. Mulders, Nucl. Phys. **A459**, 525 (1986).

[17] G. G. Simon *et al.*, Phys. Rev. Lett. **37**, 739 (1976).

[18] B. Parker *et al.*, Phys. Rev. C **34**, 2354 (1986).

[19] J. M. Laget, Can. J. Phys. **62**, 1046 (1984).

[20] W. Leidemann and A. Arenhövel, Nucl. Phys. **A393**, 385 (1983).

[21] J. S. McCarthy, I. Sick, R. R. Whitney, and M. R. Yearian, Phys. Rev. C **13**, 712 (1976).

[22] B. Blankleider and R. M. Woloshyn, Phys. Rev. C **29**, 538 (1984).

[23] H. Meier, Ch. Hajduk, P. U. Sauer, and W. Theis, Nucl. Phys. **A395**, 332 (1983).

[24] C. Marchand *et al.*, Phys. Lett. **153B**, 29 (1985).

[25] J. M. Laget, Phys. Lett. **151B**, 325 (1985).

[26] B. P. Quinn *et al.*, Phys. Rev. C **37**, 1609 (1988).

[27] B. P. Quinn, Ph.D thesis, MIT, 1984.

[28] Y. S. Tsai, Stanford Linear Accelerator Report, 848, 1971; L. W. Mo and Y. S. Tsai, Rev. Mod. Phys. **41**, 205 (1969).

[29] J. W. Motz, H. Olson, and H. W. Koch, Rev. Mod. Phys. **41**, 581 (1969); Y. S. Tsai *ibid.* **46**, 815 (1974).

[30] C. Ciofi degli Atti, E. Pace, and G. Salme, Phys. Lett. **127B**,

303 (1983).
[31]E. J. Moniz, Phys. Rev. **184**, 1154 (1969).
[32]G. Höhler *et al.*, Nucl. Phys. **B114**, 505 (1976).
[33]C. Ciofi degli Atti, E. Pace, and G. Salme, Phys. Lett. **141B**, 14 (1984).
[34]R. A. Brandenburg *et al.*, Phys. Rev. C **12**, 1368 (1975).
[35]J. M. Laget, private commuication.
[36]T. deForest and J. D. Walecka, Ann. Phys. **15**, 1 (1966).
[37]R. Schiavilla, *et al.*, Nucl. Phys. **A473**, 267 (1987); R. Schiavilla and V. R. Pandharipande, Phys. Rev. C **36**, 2221 (1987).
[38]K. A. Dow *et al.*, Bull. Am. Phys. Soc. **32**, 1052 (1987); K. F. von Reden *et al.*, *ibid.* **32**, 1059 (1987).